Tuijin Jishu/Journal of Propulsion Technology
ISSN: 1001-4055
Vol. 45 No. 2 (2024)

Cardiovascular Health Monitoring with IoMT, ML, and FBG Sensors in Operation

[1]Maitri Mohanty, [2] Premansu Sekhara Rath, [3]Ambarish G. Mohapatra

[1, 2,] Department of Computer Science and Engineering, GIET University, Gunupur, Odisha, India

[3,] Electronics Engineering, Silicon Institute of Technology, Silicon University, Bhubaneswar, Odisha, India

Abstract: In today's healthcare industry, it is essential to continuously monitor cardiac parameters and Heart Rate Variability (HRV), necessitating systems that function effectively around the clock. Therefore, the emergence of the Internet of Medical Things (IoMT) technology provides a useful approach by employing various kinds of sensors for remote monitoring and analysis. This study presents a passive optical Fiber Bragg Gratings (FBG) sensor as a promising new technology for continuous monitoring of HRV and vital sign parameters. It also incorporates machine learning techniques to forecast heart conditions, improving the efficacy of remote monitoring systems.

Method: The study methodology utilizes an in-depth structural analysis approach employing finite element analysis to examine a specialized FBG sensor. This fabricated sensor demonstrates its ability to record cardiac signals in real-time. The key cardiac parameters such as Root Mean Square of Successive Differences (RMSSD), Heart Rate (HR), Standard Deviation of Normal-to-Normal (SDNN) intervals, percentage of successive NN intervals differing by more than 50 ms (pNN50), and real-time Body Temperature are extracted from the acquired FBG signal using sophisticated signal processing algorithms. Integrating machine learning models like the Radial Basic Function Neural Network (RBF) and Partial Least Square Regression (PLSR) offers valuable insights for early detection and management of heart disease.

Findings: The outcomes of various HRV parameters, including SDNN, HR, the percentage of consecutive NN intervals that are more than 50 ms apart, and RMSSD, obtained from the proposed FBG-based sensing system compared to a Standard Heart Variability monitor, result below 10% error. Moreover, among the RBF and PLSR models, RBF stands out for its significant success, delivering clinically acceptable metrics such as R-squared error and RMSE.

Novelty: Due to its passive nature, the FBG sensor can be vulnerable to various hazardous environments such as electromagnetic radiation and corrosive atmospheres. However, FBG sensors transmit signals through optical fibers; they can be employed for remote sensing in challenging conditions where conventional electrical sensors might fail. This approach is also innovative due to the fusion of state-of-the-art FBG sensors with an IoT-based decision support system, enabling seamless 24/7 continuous monitoring of cardiac parameters and HRV in real-time scenarios.

Keywords: *IoMT, Fiber Bragg Grating, PDMS, HRV, Machine Learning, DSS, heart disease.*

1. Introduction:

In today's healthcare landscape, continuous monitoring of vital signs and HRV is imperative for patient care [1]. With the increasing prevalence of cardiovascular diseases, there is a growing demand for innovative solutions that can offer real-time insights into cardiac health [2]. Leveraging various sensors, IoMT facilitates the collection of vital physiological information, including respiration rate and HRV parameters, in real-time [3]. However, the accuracy and reliability of remote monitoring systems heavily depend on the quality of sensor data. Motion artifacts and noise often disrupt sensor signals, necessitating robust preprocessing techniques to ensure data integrity [3]. Furthermore, the convergence of FBG sensors with IoMT-based by harnessing machine learning algorithms, these systems can analyze sensor data and provide actionable insights to healthcare professionals. This paper discusses the integration of FBG vibration sensors into a decision support system, outlining a cutting-edge strategy for real-time monitoring of cardiac parameters. FBG sensors offer precision and immunity to electromagnetic interference, making them an ideal choice for monitoring cardiac

conditions in harsh environment [4]. This article disperses findings on an eight-fold higher ratio of signal to noise observed within the pulse wave signal from FBG optical sensor made with plastic optical fiber in comparison to those made with silica optical fiber [10]. The monitoring of respiration rate, PCG, and ACG using a cloth-based setup is showcased [11]. Incorporating FBG sensor data into decision support systems enables healthcare organizations to leverage advanced analytics for detecting cardiac patterns and optimizing healthcare service. To enhance preprocessing techniques, evaluate the cost-effectiveness of integrating FBG sensors into decision support systems for continuous real-time cardiac parameter monitoring, this study scrutinizes the objectives, methodologies, outcomes, and innovations associated with incorporating FBG vibration sensors into a DSS. From the preceding discussions, the research gaps and avenues for further exploration emerge as follow:

a) **Approaches for Alleviating Artifacts and Other Influential Factors:** The study highlights the influence of environmental noise, fiber coupling, and motion artifacts on FBG sensor signals, and introduces a robust preprocessing technique to mitigate these effects. However, further research is focused to enhance and refine the preprocessing approach to effectively manage a broader range of noisy signatures, to ensure data integrity, enhance diagnostic capabilities, and facilitate early intervention.
b) **Evaluation and analysis of sensor data:** The study employs a range of machine learning algorithms to analyze and interpret sensor data. Exploring algorithms to identify the most efficient and effective methods for detecting different cardiac rhythms and provides the healthcare service at earliest.
c) **Integration with Healthcare Sector:** Incorporating cardiac monitoring data from IoMT devices and FBG sensors, Electronic Health Records (EHR) can accelerate comprehensive health management and streamline record-keeping. It would be useful to investigate ways that monitoring systems and EHR platforms could work together effortlessly.
d) **Real-World Implementation and Scalability:** The study presents a practical approach through an experimental case study; however, a research gap exists in evaluating the scalability and real-world implementation of the proposed integrated FBG sensor-DSS system across a range of healthcare setups. Decision support system represents a significant advancement in cardiac monitoring. Assessing the system's performance in diverse operational conditions and different healthcare sectors will validate its effectiveness and practicality on a larger scale.

Here, this study advances real-time healthcare solutions by facilitating data collection and transmission, enabling continuous monitoring through biocompatible FBG sensors. It harnesses Machine Learning algorithms for analytics, detecting anomalies and diagnosing heart conditions. Integrating DSS assists healthcare providers in making informed decisions based on analyzed data and predefined rules, as depicted in Figure 1. This transformative approach, driven by FBGs, enhances healthcare infrastructure, offering effective solutions even in demanding circumstances.

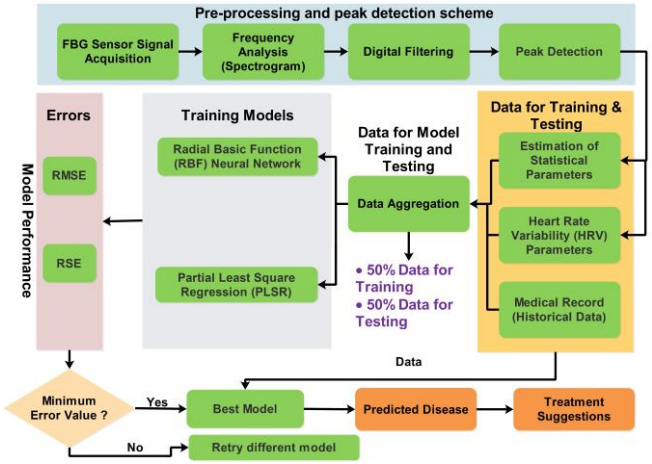

Figure 1: Block schematic of the suggested FBG sensor-based IOMT-based cardiac monitoring system

This article introduces a methodology to implement an integrated IoT-enabled cardiac monitoring system using FBG sensors. The article is organized into ten sections to emphasize FBG sensing-based IoMT healthcare systems for monitoring cardiac parameters. It begins with a discussion of the work's scope, followed by a

comprehensive literature review. The methodology is covered in the fourth section, along with its limitations. The goals of the method are highlighted in the sixth section, and the working principle of the FBG sensor is detailed in the seventh section. The experimental setup is described in the eighth section, followed by the presentation of experimental results and discussions. Finally, the last section summarizes the conclusions of the proposed work, outlines prospects, and provides references.

2. Scope of the Work

The study offers a thorough explanation of the way FBG vibration sensors can be integrated into a DSS and outlines a cutting-edge technique for monitoring heart parameters in real-time situations. This proactive strategy maximizes healthcare service, identifies various cardiac rhythms, and provides early disease identification, which help practitioners to save lives. By enabling the seamless transmission of sensor data to healthcare professionals, the use of FBG vibration sensors, IoMT, and advanced algorithms of machine learning holds the promise of facilitating remote patient monitoring and addressing the limitations of the traditional healthcare business. The proposed research work encompasses two main scopes:

- **Continuous Remote Cardiac Monitoring:** The research demonstrates that FBG sensors, renowned for their precision and immune to electromagnetic interference, effectively and continuously monitor a range of cardiac and vital sign parameters. Integrated with IoMT, they enable seamless data transmission to healthcare practitioners, facilitating remote patient monitoring and improving healthcare service accessibility regardless of the patient's location.
- **Advanced Decision Support System for Early Detection of Health Conditions:** This study highlights the feasibility of personalized healthcare interventions based on individual patient data through the real-time integration of FBG sensors with IoMT and DSS. With the use of machine learning algorithms within DSS to analyze the data gathered from FBG sensors, medical professionals can detect potential cardiac abnormalities and abnormal cardiac patterns early on. This enables timely intervention and management of cardiac conditions, resulting in better patient outcomes. This FBG-based sensing system with cutting-edge technology can be deployed effectively to meet the evolving needs of the healthcare industry.

3. Literature Review

This literature survey highlights various studies exploring advancements in FBG sensor technology, IoT, ML, and their applications in healthcare industry. Notably, to monitor cardiovascular pulse parameters in real-time, Shi et al. (2023) [3] present a small, incredibly accurate force-sensitive flexure (FBG) sensor with a sensitivity of 1547.3 pm/N. This sensor effectively translates longitudinal pulse input. At the same time, F. De Tommasi et al. (2023) [4] investigate the use of 13-FBG array mattresses with FBG sensors for non-invasive cardiorespiratory monitoring, which indicated promising accuracy in continuous heart rate calculations under various circumstances. Additionally, X. Wang et al. (2022) [5] showcase FBG sensor resilience, providing a body temperature monitoring vest with waterproof, resistive to electromagnetic waves FBG sensors, suitable for scenarios such as MRIs and ultrasounds. Moreover, Ladrova et al. (2022) [6] investigate MRI incorporating FBG sensors for cardiovascular monitoring, addressing challenges like signal delays. Further, M. Krej et al. introduced a mat of sensors with nine arrays of FBG sensors, positioned orthogonally within a single-mode fiber, placed on a flexible Plexiglas board for heart rate data collection from multiple locations (2021) [7]. Also employ decimation and bandpass filters for preprocessing the acquired BCG signal. In (2020) [8], Xin Cheng builds a Polymer Optical Fiber Bragg Grating (POFBG) sensor using UV laser light pulse exclusively on ZEONEX-based POFS, demonstrating the sensor's ability to distinguish exhalation and inhalation during human breathing holds. The sensor additionally employs a deep-learning Temporal Convolution Network (TCN) for heart rate detection. According to Shouhei Koyama and Hiroaki Ishizawa, an FBG sensor is placed near a person's wrist radial artery, and the recorded signal is filtered to compute respiratory rate (RR) and heart rate (HR) using the Complete Ensemble empirical Mode Decomposition with Adaptive Noise (CEEMDAN) method (2019) [9] Y. Haseda et al. (2019) [10] show that silica and plastic optical fibers are utilized in the FBG sensor fabrication, with the signal filtered between 0.5 and 5.0 Hz, and PLSR(Partial Least Square Regression) techniques employed in compute pulse waves and blood pressure readings, revealing an eight-fold rise in the signal-to-noise ratio in the FBG sensor's pulse wave signal made of plastic optical fiber compared to silica optical fiber. Also, Ogawa et al. propose a cloth-based setup for monitoring respiration signals, PCG, and ACG (2018) [11]. Moreover, setups by Nedoma et al. (2018) [12] and

Sadek et al. (2015) [113] focus on biocompatible setups for HR and BCG signal detection. Furthermore, Zhu et al. (2014) [14] present FBG configurations for HR measurement using cepstrum analysis. Collectively, these studies offer insights into real-time healthcare monitoring systems utilizing sensor technologies illustrated in Table 1.

Table 1: Relevant literature and limitations of proposed methodologies

Study	Utilizing techniques for parameter extraction	Limitations
Shi et al. (2023) [3].	Compact six-bar parallel mechanism of FBG sensor for HR monitoring.	Insufficient discussion about IoMT-based FBG sensors.
F. De Tommasi et al. (2023) [4].	FBG sensors show promising heart rate accuracy.	Limited discussion on the scalability and adaptability of the system.
X. Wang et al. (2022) [5]	FBG sensors show body temperature against various conditions .	Limited information on cost-effectiveness.
Ladrova et al. (2022) [6]	Monitoring cardiorespiratory parameters during MRI, addressing challenges like signal delays. .	Scalability and long-term performance not discussed
M. Krej et al. (2021) [7]	Decimation and bandpass filters are used for preprocessing and detects HR.	The study may not provide insights into dependability and the durability over a longer period of sensors.
Xin Cheg et al. (2020) [8].	Distinguish the exhalation and inhalation of the human respiration process while breath holds.	Fewer data on model generalization.
S. Koyama and H. Ishizawa (2019) [9].	Measurement of HR and RR is accomplished using the CEEMDAN (Complete Ensemble Empirical Mode Decomposition with Adaptive Noise) method.	Fewer data on model generalization.

Although the literature analysis offers a thorough understanding of FBG sensor technologies and cardiac parameter monitoring, there is a glaring research gap regarding integrating FBG sensors with machine learning-driven DSS. This integration can potentially furnish healthcare professionals with actionable insights and decision support derived from real-time FBG sensor data. Furthermore, additional research is needed to explore novel applications and developments in the integration of cutting-edge technologies into FBG sensors, with an emphasis on scalability, accuracy, and practical deployment. These technologies include the Internet of Things (IoT), advances in polymer engineering, Data Analytics, Digital Signal Processing, and DSS. By providing practical concepts for improved healthcare services system strategies in healthcare Industry 4.0, closing these gaps will make progress the healthcare industry.

4. Methodology

The methodology addresses sensor placement, data collection, analysis, interpretation, and decision-making are systematically done by this technique, which is illustrated in Figure 2.

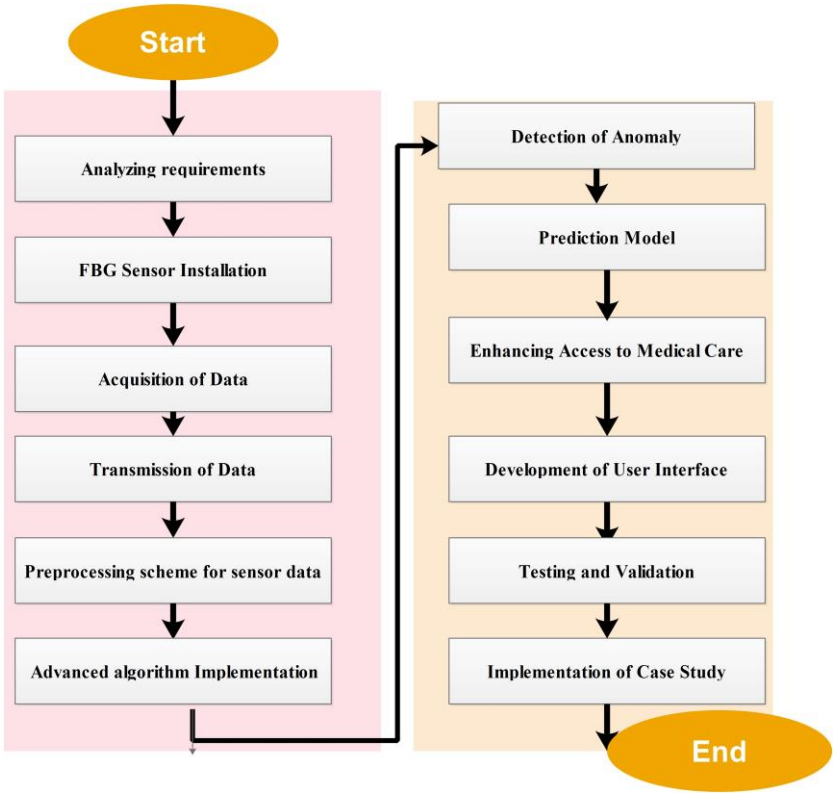

Figure 2: The systematic approach of the Methodology

In the integration of FBG sensors for cardiac monitoring, several key steps are undertaken. Initially, requirements are analyzed to identify suitable medical equipment and establish data collection parameters. FBG sensors are then meticulously installed on chosen cardiac monitoring devices, considering factors like sensor positioning and attachment techniques to ensure precision. A real-time data collection system is developed to gather cardiac data from the installed FBG sensors, utilizing optical interrogators to track wavelength shifts and correlate them with cardiac dynamics. Reliable data transfer to a centralized database or cloud platform for analysis and storage has been established. Preprocessing schemes are applied to normalize and align sensor data, enhancing accuracy for subsequent analysis. Subsequently, a decision support system is built; incorporating FBG sensor data for cardiac anomaly identification and early disease detection. Advanced algorithms, including machine learning methods, are implemented for in-depth cardiac data analysis, anomaly detection, and prediction modeling. By prioritizing monitoring tasks according to the likelihood and severity of anomalies, the system aims to improve access to healthcare services. A user-friendly interface is developed to provide medical personnel with real-time sensor data visualization, anomaly alerts, and predictive insights. To ensure system performance and dependability under varied circumstances, thorough testing and validation procedures have been carried out. Finally, a comprehensive case study is conducted in a cardiac monitoring setting to validate the system's ability to identify irregularities and forecast events over a specified timeframe.

5. Limitation of Methodology

Remote monitoring of IoMT-based FBG sensing schemes faces inherent limitations due to challenges in achieving distributed sensing of cardiac and respiratory parameters in continuous real-time monitoring environments like specialized ICUs. Calibration and signal processing of FBG sensor elements pose further obstacles, exacerbated by difficulties in ensuring reliable data transfer to DSS amidst signal loss or electromagnetic interference. Computational complexity and reliance on EHR for predictive model development add additional layers of complexity, highlighting the need to address these challenges to optimize performance in practical healthcare settings.

6. Objective of Proposed Method

This innovative approach introduces an advanced cardiac monitoring system for the healthcare industry by integrating FBG vibration sensors into a decision support system. The primary objective is to establish a framework for early detection of potential cardiac abnormalities and irregular patterns, enabling real-time decision-making through the utilization of high-precision data collected by FBG sensors. The research endeavors to develop a robust DSS capable of generating relevant alerts during medical emergencies by effectively managing intricate cardiac data. Evaluation will involve assessing precision, validity, sensitivity, and the system's capacity to deliver timely alerts and support early detection of heart disease.

7. Working Principle of Fiber Brag Grating Sensor (FBG)

FBG technology stands out among optical fiber sensors for its straightforward manufacturing process and significant efficacy based on light reflection principles. In generating FBGs, the fiber core's longitudinal refractive index undergoes regular modulation, relying on the theory of diffraction gratings [4]. Grating refers to the periodic alteration of the optical fiber core's refractive index. As broadband light traverses the grating surface along the longitudinal axis, some light reflects while the remainder continues through the fiber. The amalgamation of reflected light produces a single, narrow reflected beam meeting the Bragg condition [4]. Consequently, this periodic configuration functions as a precise wavelength filter. External influences, such as strain and temperature, affect the FBG, causing fluctuations in refractive index and pitch periodicity directly linked to changes in Bragg wavelength, which is explained in equation 1.

$$\lambda\_B = 2\eta\_eff\ \Lambda \quad (1)$$

Where η_eff represents the optical fiber effective inner refractive index, Λ stands for the grating period, which determines distance between two neighbouring grating planes, and, and λ_B denotes the Bragg peak wavelength [15]. The working principle of FBG is explained and represented in Figure 3.

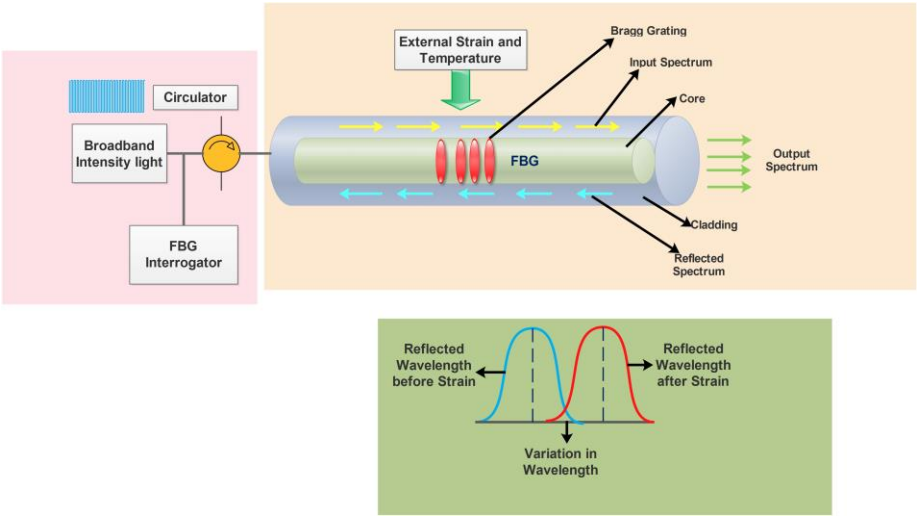

Figure 3: Basic operational principle of FBG

Equation 2 extends on this concept elucidating the dependence of peak wavelength shift λ_B, on both applied temperature (ΔT) and strain (ε).

$$\frac{\Delta\lambda_B}{\lambda_B} = \left(\frac{1}{\Lambda}\frac{\partial\Lambda}{\partial\Sigma} + \frac{1}{\eta_{eff}}\frac{\partial\eta_{eff}}{\partial\Sigma}\right)\Delta\Sigma + \left(\frac{1}{\Delta}\frac{\partial\Lambda}{\partial T} + \frac{1}{\eta_{eff}}\frac{\partial\eta_{eff}}{\partial T}\right)\Delta T \quad (2)$$

Equations 3 and 4 encapsulate the effect of strain on the peak Bragg wavelength, with temperature held constant

$$\frac{\partial\eta_{eff}}{\eta_{eff}} = \eta_{eff}^2[P_{12} - \nu(P_{11} - P_{12})] \quad (3)$$

$$P_e = \frac{\eta_{eff}^2}{2}[P_{12} - \nu(P_{11} + P_{12})] \quad (4)$$

Equation 5 presents the change in peak Bragg wavelength, influenced by the coefficient of optical strain in the fiber P_e which is expressed as a function of optical strain components P_{ij}, Poisson's ratio (V), and the refractive index (η_{eff}).

$$\Delta\lambda_B = (1 - P_e)\lambda_B \Sigma \quad (5)$$

Equation 6 elucidates the impact of temperature variations on the peak Bragg wavelength when strain is maintained at zero.

$$\Delta\lambda_B = \lambda_B \left(\frac{1}{\eta_{eff}}\frac{\partial \eta_{eff}}{\partial T} + \frac{1}{\Lambda}\frac{\partial \Lambda}{\partial T}\right)\Delta T \quad (6)$$

Equation 7 defines the change in peak Bragg wavelength, influenced by coefficients α and β, which are determined by derivatives of refractive index and pitch, correlating with temperature variations.

$$\lambda_B(\alpha + \beta)\Delta T = K_T \lambda_B \Delta T \quad (7)$$

Equations 8, 9, and 10 unveil the combined influence of the thermal expansion coefficient (α) and the thermo-optic coefficient (β) on the sensor's response to temperature fluctuations, demonstrating their cumulative effect.

$$\alpha = \frac{1}{\Lambda}\frac{\partial \Lambda}{\partial T} \quad (8)$$

$$\beta = \frac{1}{\eta_{eff}}\frac{\partial \eta_{eff}}{\partial T} \quad (9)$$

$$K_T = \alpha + \beta \quad (10)$$

These formulas can be used by scientists and engineers to create precise and efficient FBG sensors for a wide range of applications, including cardiovascular monitoring and other disciplines.

8. FBG Experimental Setup

The sensor component is manufactured in a controlled laboratory environment using PDMS. Within PDMS, the FBG optical sensor is integrated to form the sensor unit. A High-speed FBG interrogator Ibsen IMON 512 and SLED illumination are utilized for interfacing. Swift cardiac waveform recording is facilitated by a dedicated PC with specific hardware. The connection between the interrogator unit and PC is enabled by a Gigabit switch. Data gathering is coordinated via the LabVIEW platform, using an exclusive DLL library. The entire laboratory setup is depicted in Figure 4. The proposed method targets dynamic strain patterns, capturing cardiac activities.FBG sensing, embedded in a wearable chest belt, detects mechanical stress from heart activity. This enables detection and measurement of various cardiac activities. Consequently, fluctuations in sensor output directly correlate with cardiac events. The resulting stress influences the FBG's period. The approach is tailored for leveraging FBG-based vital-sign sensors. It focuses on capturing heart sounds and other motion artifacts. Thus, it provides a comprehensive method for monitoring cardiac activity.

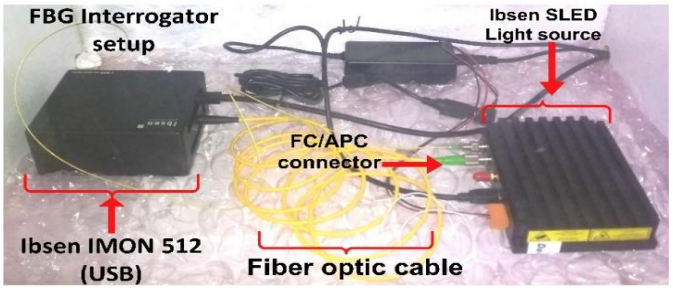

Figure 4: Experimental setup of the FBG Interrogator

In a laboratory environment, we conducted a thorough experimental investigation involving three healthy participants and one subject with arrhythmias, aged between 30 and 60 years, including two males and two

females. By sampling the FBG at an impressive rate of 1000 times per second within the wavelength range of 1550 to 1560mm, with a resolution of 1 pm, we achieved a comprehensive understanding of cardiac dynamics. Nevertheless, the cardiac signals obtained are vulnerable to various artifacts such as motion disturbances, environmental noise, and coupling effects.

9. Results and Discussions

The FBG-based sensor captured real-time cardiac signals, though susceptible to interferences like motion disturbances, environmental noise, and coupling effects. These interferences overlay the genuine cardiac signature with low-amplitude, high-frequency baseline noise. Figures 5 and 6 depict the raw signals captured from four subjects.

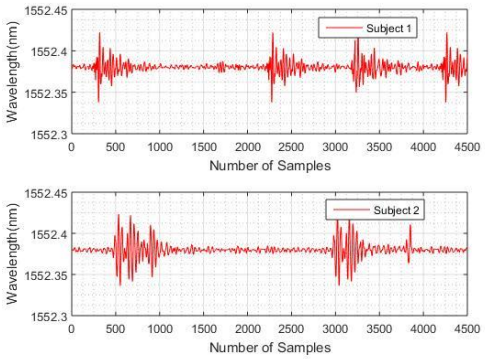

Figure 5: Cardiac Raw Signal of Subject 1 and Subject 2

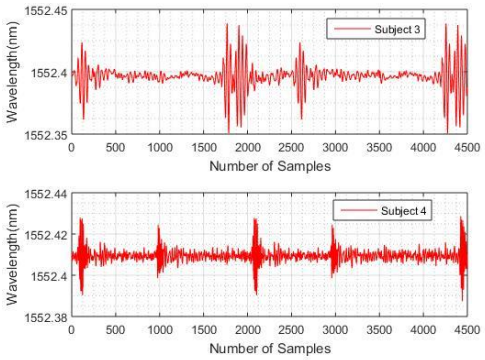

Figure 6: Cardiac Raw Signal of Subject 3 and Subject 4

To address noise, identifying noise frequencies within the signal is crucial. Spectrograms provide insight into frequency elements over time, aiding in pattern recognition. Utilizing Fast Fourier Transformation (FFT) precisely locates these frequencies for further processing; Figures 7-8 depict FFT representations of the unprocessed cardiac signal.

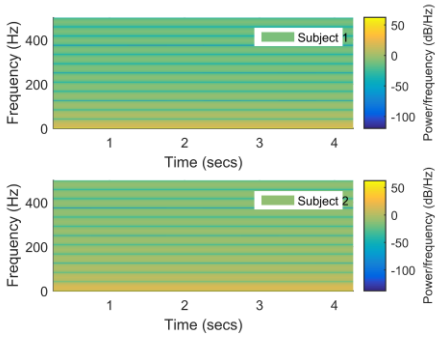

Figure 7: Spectrogram of Subject 1 and Subject 2

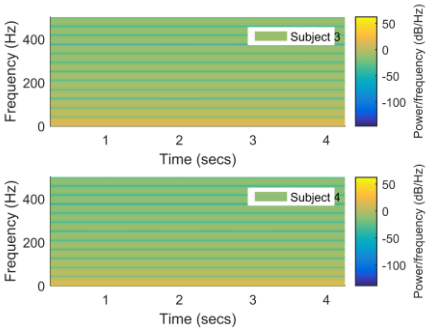

Figure 8: Spectrogram of Subject 3 and Subject 4

In initial FBG signal, noise frequencies below 10 Hz and above 140 Hz are present. Addressing this, a straightforward method involves applying a moving average filter, smoothing abrupt fluctuations and high-frequency noise. Additionally, a custom-designed Infinite Impulse Response (IIR) bandpass filter selectively preserves the essential cardiac frequency range while effectively removing undesired low and high-frequency components, as demonstrated in Figures 9 and 10.

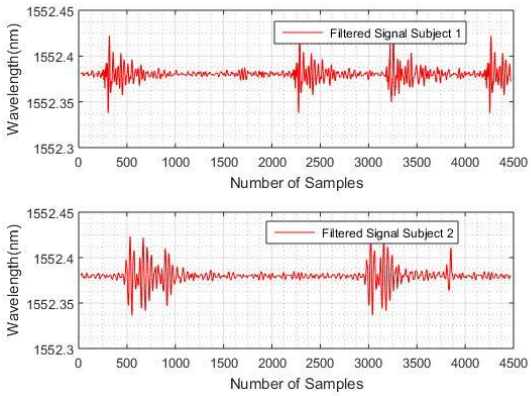

Figure 9: Signal filtration for subjects 1 and 2.

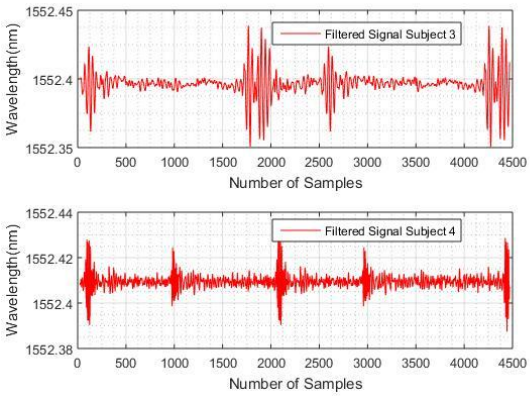

Figure 10: Signal filtration for subjects 3 and 4.

Group delay, linked to the phase response of a filter, measures the amount of time it requires for the frequency elements to pass through the filter. When filtering signals, especially complex signals, addressing the subtleties of group delay is essential; variations can distort filtered signals. When designing or choosing noise reduction filters, mindful consideration of group delay is vital to preserve temporal signal information, as depicted in Figures 11.

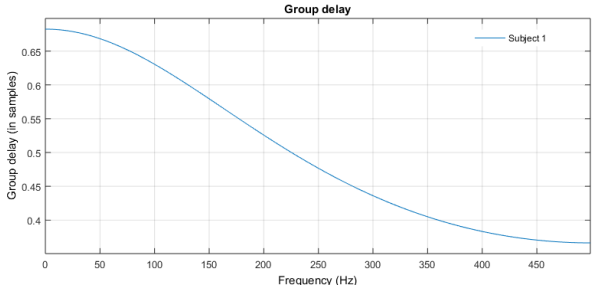

Figure 11: Group delay of Subject 1

After the filtration process, a specialized peak detection algorithm becomes essential. It detects precisely the peaks corresponding to individual heartbeats in the 1545.7–1545.9 nm output wavelength location of the FBG sensor. The peaks are essential indicators for evaluating HRV standards such as HR, SDNN, and RMSSD. Visual representations in Figures 12 to 15 illustrate the peaks extracted from the filtered FBG signal.

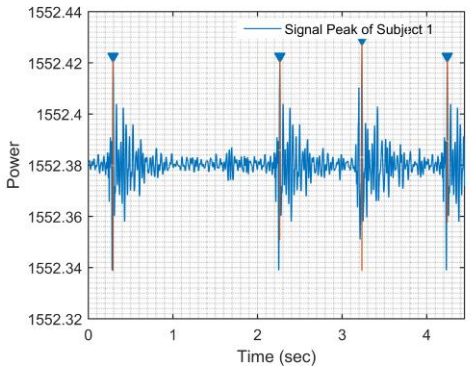

Figure 12: Subject 1's Peak Signal

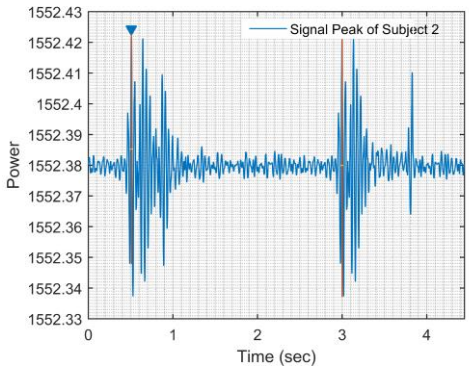

Figure 13: Subject 2's Peak Signal

.

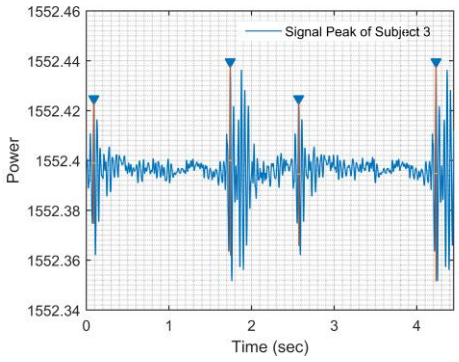

Figure 14: Subject 3's Peak Signal

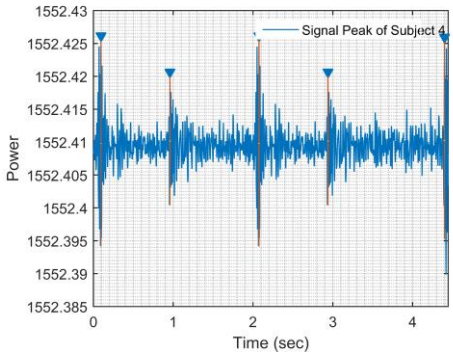

Figure 15: Subject 4's Peak Signal

Furthermore, HRV specifications including HR, RMSSD, SDNN, and pNN50 for a normal person is presented in Tables 2.

Table 2: HRV Measurements for a Normal Individual

Cardiac Parameters	Age Range	Cardiac Condition	Range of Parameters
Mean Heart Rate [15]	30.0-65.0	No Disease	Minimum=55 beats/ minute Maximum=105 beats/minute
Standard Deviation of Normal-to-Normal intervals [16]	30.0-65.0	No Disease	Minimum=20.4miliseconds Maximum=51.4milisseconds
Root Mean Square of Successive Differences [16]	30.0-65.0	No Disease	Minimum=11.7miliseconds Maximum=42.9miliseconds
Proportion of consecutive NN intervals differing by more than 50 ms [15]	30.0-65.0	No Disease	Minimum=3%Maximum=23%

The parameters Δ_{mxh} and Δ_{mnh} denote the maximum and minimum wavelength shifts, respectively, representing the deviation from the base wavelength of the FBG sensor. These notations are formally defined in Equation 11 and Equation 12.

$$\Delta_{mxh} = \lambda_{max} - \lambda_B \quad (11)$$

$$\Delta_{mnh} = \lambda_{min} - \lambda_B \quad (12)$$

Here, λ_{max} represents the maximum wavelength in the FBG signal post-filtering stage, and λ_{min} denotes the minimum wavelength in the FBG signal post-filtering stage. Moreover, statistical parameters like Maximum Height, Minimum Height, Mean, and Sigma of the signal are calculated to enrich the analysis, as outlined in Table 3.

Table 3: Different Statistical Parameters of Cardiac signal of subjects in the experiment

Subjects	Δ_{mxh} (nm)	Δ_{mnh} (nm)	Mean(nm)	Sigma
1	1552.4094	1551.8596	1552.1028	0.0534
2	1552.4094	1551.8596	1552.1028	0.0534
3	1552.4064	1552.2677	1552.3316	0.0136
4	1552.4060	1552.3571	1552.3819	0.0050

Table 4 shows the health condition of the subjects involved in the experimental study.

Table 4: Subjects involved in the experiment for Health condition Status

Subjects	Age	Sex	Subject Health Status
1	42	M	Normal Person
2	40	F	Normal Person
3	42	F	Normal Person
4	41	M	Arrhythmia

In the experimental study, Table 5 displays the recorded HRV parameters of subjects captured by both the FBG sensor and the Standard HRV monitor.

Table 5: Subjects involved in the experiment with recorded Cardiac Parameters by FBG sensor and Standard HRV monitor

Subjects	HRV parameters recorded by FBG Sensor				HRV parameters recorded by Standard HRV monitor				Percentage of Error
	HR (bps)	SDNN (ms)	RMSSD (ms)	pNN50 (%)	HR (bps)	SDNN (ms)	RMSSD (ms)	pNN50 (%)	
1	60.52	37.34	22.42	3.25	65.50	40.32	24.20	3.50	7%
2	61.25	37.5	30.75	3.75	65.50	40.22	33.0	4.00	6%
3	63.01	37.14	30.59	4.75	66.15	39.35	32.2	5.00	5%
4	52.25	36.29	28.5	4.2	55.00	38.2	30.1	4.5	5%

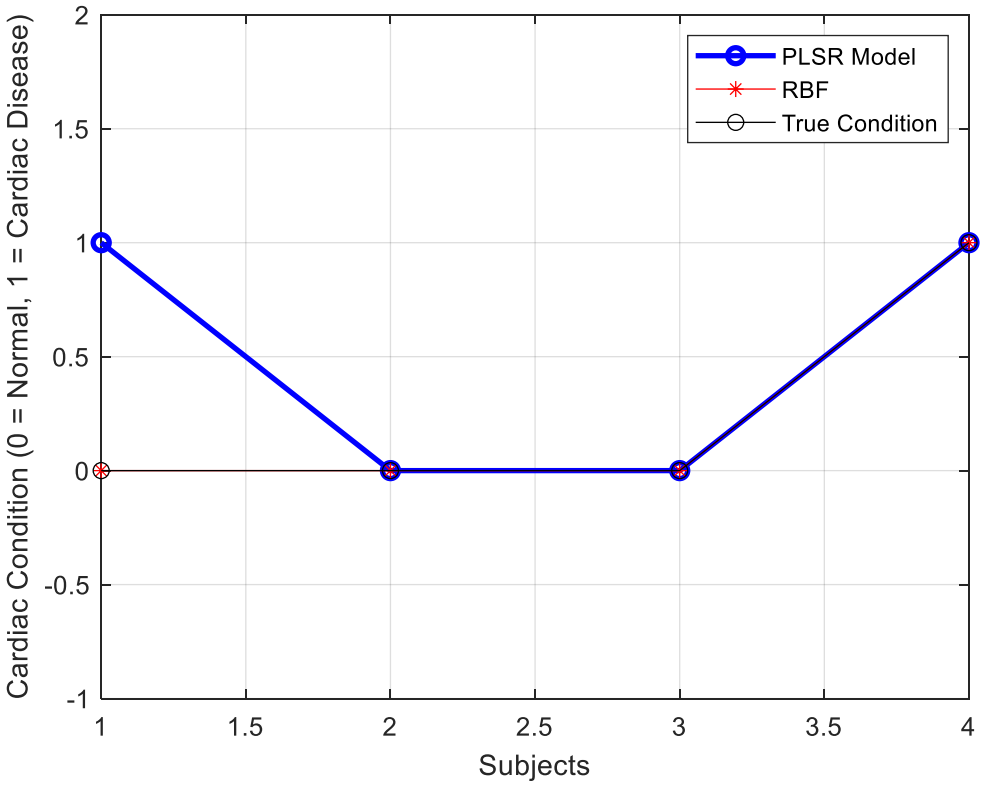

Figure 16. Cardiac disease estimation using PLSR and RBF

Table 6 shows the evaluation of errors using machine learning models subjects involved in the experimental study.

Table 6: Evaluation of machine learning models based on error

Models	**Membership function/ Activation Function**	**Training Data Set**		**Testing Data Set**	
		RMSE	**R-squared**	**RMSE**	**R-squared**
The Radial Basic Function Neural Network (RBF)	Product of two sigmoidal membership functions	0.000282	0.999	0.000278	0.999
	Gaussian combination membership function	0.000283	0.998	0.000274	0.997
	This function uses a sigmoidal membership function to compute fuzzy membership values.	0.000280	0.997	0.000276	0.997

Partial Least Square Regression (PLSR)		0.53852	0.911207	0.53860	0.911227

Furthermore, the diverse models possess the capability to extract complex patterns and correlations from processed data, improving comprehension of cardiac dynamics, anomaly detection, and proactive healthcare management. The evaluation of the pre-processing pipeline's effectiveness employs two crucial performance metrics to ensure accurate insights: Root Mean Square (RMS) error and R-squared (R^2) error. The dataset is split into 50% for training and 50% for testing to ensure robustness. Radial Basic Function Neural Network (RBF) shows outstanding performance, with low RMSE values (0.000280 to 0.000283) and high R-squared values (0.997 to 0.999) in both datasets. Conversely, Partial Least Square Regression (PLSR) with Gaussian activation function exhibits moderate performance, with RMSE values around 0.53852 in training and 0.53860 in testing, along with corresponding R-squared values of about 0.911207 and 0.911227. However, PLSR's accuracy and predictive power are notably lower compared to RBF neural network. The figure 16 shows a comparative analysis on the performance of the proposed prediction models (PLSR and RBF). Table 7 illustrates the performance evaluation of various models.

Table 7: Evaluation of machine learning models based on error

Models	**Performance Analysis**	**Model Selectivity**
The Radial Basic Function Neural Network (RBF)	• Low RMSE values Training dataset=0.000280 to 0.000283. Testing dataset=0.000274 to 0.000278. • High R-squared values Training data set=0.996 to 0.999. Testing data set=0.997 to 0.999.	• High accuracy and predictive capability. • It consistently attains the lowest RMSE and highest R-squared values across different membership functions/activation functions.
Partial Least Square Regression (PLSR)	• RMSE values Training dataset=0.53852 Testing dataset=0.53860 • R-squared values Training dataset=0.911207 Testing dataset=0.911227.	• Moderate performance compared to the RBF neural network.

10. Conclusion

This study demonstrates the successful implementation of IoMT-based FBG sensing technology, with Machine Learning (ML) playing a crucial role in its architecture. Extensive Finite Element Analysis is conducted to design the FBG sensing element, incorporating detailed structural analysis to enhance sensitivity using PDMS polymer. The FBG sensing system facilitates the detection of cardiac patterns and anomalies, enabling early disease detection and optimizing healthcare service delivery to save lives. It offers real-time cardiac monitoring through a comprehensive methodology integrating sensor deployment, data analysis, and user interface design. Leveraging the IoMT framework and cloud computing, it enables real-time tracking of various cardiovascular parameters for multiple patients, facilitating remote monitoring and early disease diagnosis.

Limitations: Although there is great potential for incorporating FBG vibration sensors into IoMT-based decision support systems, there are many challenges to overcome, including high cost of sensor deployment, the complexity of developing algorithms, as well as potential data security issues. The efficacy of the technique is dependent upon the precision of sensor calibration and the availability of previous data. Further, additional study is needed to determine the long-term dependability and longevity of FBG sensors for continuous cardiac monitoring, which raises challenges regarding their capacity to work consistently over long periods.

Future scopes: Future efforts could prioritize enhancing signal processing algorithms for improved precision in deriving essential cardiac parameters from FBG sensors. Additionally, conducting comprehensive and prolonged reliability studies to enhance healthcare operations' resilience and adaptability, exploring AI-driven decision support systems, and establishing standard procedures to guarantee uniformity and comparability across different research initiatives and medicinal applications would be beneficial.

Acknowledgements: The authors would like to express their appreciation to the Silicon Institute of Technology, Bhubaneswar, and the Central Glass and Ceramic Research Institute (CGCRI), Kolkata for their unwavering cooperation in the fabrication of the FBG optical sensor throughout the research period. Furthermore, the authors extend their appreciation to the Silicon Institute of Technology, Bhubaneswar for providing essential licensed software, including LabVIEW and FBG interrogator, which acted an essential function in the successful execution of this experiments.

References

[1] R. Rohan, K. Venkadeshwaran, and P. Ranjan, "Recent advancements of fiber Bragg grating sensors in biomedical application: a review," J. Opt., vol. 53, no. 1, pp. 282-293, 2024.
[2] C. Massaroni, M. Zaltieri, D. L. Presti, A. Nicolò, D. Tosi, and E. Schena, "Fiber Bragg grating sensors for cardiorespiratory monitoring: A review," IEEE Sens. J., vol. 21, no. 13, pp. 14069-14080, 2020.
[3] C. Shi, H. Zhang, X. Ni, and K. Wang, "An FBG-Based Sensor with Both Wearable and Handheld forms for Carotid Arterial Pulse Waveform Measurement," IEEE Trans. Instrum. Meas., 2023.
[4] F. De Tommasi, C. Massaroni, M. A. Caponero, M. Carassiti, E. Schena, and D. L. Presti, "FBG-based Mattress for Heart Rate Monitoring in Different Breathing Conditions," IEEE Sens. J., 2023.
[5] X. Wang, Y. Jiang, S. Xu, H. Liu, and X. Li, "Fiber Bragg grating-based smart garment for monitoring human body temperature," Sensors, vol. 22, no. 11, p. 4252, 2022.
[6] M. Ladrova, J. Nedoma, R. Martinek, K. Behbehani, and R. Kahankova, "Fiber-Optic Cardiorespiratory Monitoring and Triggering in Magnetic Resonance Imaging," IEEE Trans. Instrum. Meas., vol. 71, pp. 1-14, 2022.
[7] M. Krej et al., "Deep learning-based method for the continuous detection of heart rate in signals from a multi-fiber Bragg grating sensor compatible with magnetic resonance imaging," Biomed. Opt. Express, vol. 12, no. 12, pp. 7790-7806, 2021.
[8] X. Cheng, D. S. Gunawardena, C. F. J. Pun, J. Bonefacino, and H. Y. Tam, "Single nanosecond-pulse production of polymeric fiber Bragg gratings for biomedical applications," Opt. Express, vol. 28, no. 22, pp. 33573-33583, 2020.
[9] S. Koyama, H. Ishizawa, and S. K. Liaw, "Vital sign measurement using FBG sensor for new wearable sensor development," in Fiber Optic Sensing-Principle, Measurement and Applications, IntechOpen, 2019, pp. 1-16.

[10] Y. Haseda et al., "Measurement of pulse wave signals and blood pressure by a plastic optical fiber FBG sensor," Sensors, vol. 19, no. 23, p. 5088, 2019.
[11] K. Ogawa et al., "Simultaneous measurement of heart sound, pulse wave, and respiration with single fiber Bragg grating sensor," in 2018 IEEE International Symposium on Medical Measurements and Applications (MeMeA), IEEE, pp. 1-5, 2018.
[12] J. Nedoma et al., "Magnetic resonance imaging compatible non-invasive fiber-optic sensors based on the Bragg gratings and interferometers in the application of monitoring heart and respiration rate of the human body: A comparative study," Sensors, vol. 18, no. 11, pp. 3713, 2018.
[13] J. Sadek, J. Biswas, V. F. S. Fook, and M. Mokhtari, "Automatic heart rate detection from FBG sensors using sensor fusion and enhanced empirical mode decomposition," in 2015 IEEE International Symposium on Signal Processing and Information Technology (ISSPIT), IEEE, pp. 349-353, 2015.
[14] Y. Zhu et al., "Heart rate estimation from FBG sensors using cepstrum analysis and sensor fusion," in 2014 36th Annual International Conference of the IEEE Engineering in Medicine and Biology Society, IEEE, pp. 5365-5368, 2014.
[15] G. M. G. C. V. M. G. M. F. Sessa and V. Anna, "Heart rate variability as a predictive factor for sudden cardiac death," Aging (Albany NY), vol. 10, p. 166, 2018.
[16] M. N. Jarczok et al., "Heart rate variability in the prediction of mortality: A systematic review and meta-analysis of healthy and patient populations," Neurosci. Biobehav. Rev., vol. 143, p. 104907, 2022.